Faraday Discuss. Chem. Soc., 1982, **73**, 153–172

Energetics and Dynamics of Large Van der Waals Molecules

BY UZI EVEN, AVIV AMIRAV, SAMUEL LEUTWYLER,*

MARY JO ONDRECHEN,† ZIVA BERKOVITCH-YELLIN ‡ AND JOSHUA JORTNER

Department of Chemistry, Tel-Aviv University, Tel Aviv 69978, Israel

Received 2nd December, 1981

We report on the synthesis, identification, excited-state energetics, interstate electronic relaxation and intrastate nuclear dynamics in electronically–vibrationally excited states of Van der Waals molecules, consisting of a large aromatic molecule bound to inert-gas atoms.

INTRODUCTION

A Van der Waals (VDW) complex, consisting of an organic aromatic molecule (M) bound to inert-gas (R) atoms [1-10] can be viewed as a " guest " molecule embedded in a well-characterized local solvent configuration. Studies of excited-state energetics and dynamics of such large VDW complexes are expected to provide basic information on solvent perturbations, as explored from the microscopic point of view. With this goal in mind, we have undertaken to explore the spectroscopy and intramolecular dynamics of electronically–vibrationally excited states of a variety of MR_n complexes, where M constitutes a substituted benzene (aniline), a medium-sized aromatic (fluorene), a large linear polyacene (anthracene, tetracene and pentacene) or a very large aromatic molecule (ovalene). In this paper, we shall focus on some of the features of these large VDW complexes, which can be classified in the following manner:

A. *Chemistry*

A.1 Formation kinetics of MR_n molecules.
A.2 Identification and characterization of the chemical composition of MR_n complexes.
A.3 Specification of chemical isomers.
A.4 Estimates of VDW binding energies.

B. *Spectroscopy*

B.1 Microscopic spectral shifts of the electronic origin of M in MR_n.
B.2 Solvent effects on intramolecular vibrations of M in MR_n.
B.3 Intermolecular vibrations of low-frequency, large-amplitude M–R motion.

C. *Intramolecular Dynamics*

C.1 Microscopic solvent effects on electronic relaxation of M in MR_n.

* Present address: Physikalisch Chemisches Institut der Universitat Basel, Klingelbergstrasse 80, 4056 Basel, Switzerland.
† Present address: Department of Chemistry, Northeastern University, Boston, Massachusetts 02115, U.S.A.
‡ Permanent adress: Department of Structural Chemistry, The Weizmann Institute of Science, Rehovot 76100, Israel.

C.2 Non-reaction intramolecular vibrational energy flow in MR_n complexes, involving both intermolecular M–R modes and intramolecular modes of M.
C.3 Reactive vibrational predissociation of large MR_n molecules.

The understanding of the structure, energetics and dynamics of large VDW molecules requires a different conceptual framework than that applied, so successfully, to small VDW complexes. In the latter case, detailed spectroscopic information on realistic potential energy surfaces can be obtained,[11-13] serving as central input data for the description of energy levels and relaxation phenomena. This approach is prohibitively difficult for large VDW complexes in view of the huge dimensionality of the potential surface. The elucidation of the features of such large VDW complexes currently rests on experimental spectroscopic information for the energetics, which is supplemented by crude model calculations of the potential surfaces for the elucidation of the structure and energetics, together with coarse-graining procedures for the description of intramolecular dynamics.

EXPERIMENTAL

The large VDW complexes were synthesized in seeded supersonic expansions,[14,15] where by an appropriate choice of the experimental conditions, *i.e.* stagnation pressure and the nozzle diameter, one can accomplish selective, gradual and controlled solvation of the aromatic molecule. The experimental interrogation techniques are based on energy-resolved and time-resolved laser spectroscopy in seeded supersonic expansions. Supersonic expansions of three types were produced: (*a*) continuous axial-symmetric jets from a circular nozzle,[14,15] (*b*) pulsed axial-symmetric jets,[8] (*c*) pulsed planar supersonic jets from a nozzle slit.[16] The rare-gas diluent at the stagnation pressure $p = 10\text{-}10^4$ Torr was mixed with the organic vapour (at pressures of 10^{-2}-1 Torr) in the heated sample chamber and sent through the nozzle. The following interrogation methods were utilized: (1) fluorescence excitation spectra,[15] corresponding to the intensity of the total fluorescence *versus* the laser wavelength, (2) energy-resolved emission spectra,[15] which correspond to the energy-resolved fluorescence resulting from excitation at a fixed laser wavelength, (3) time-resolved emission,[15] corresponding to time-resolved fluorescence excited at a fixed laser wavelength, (4) energy-resolved and mass-resolved spectroscopy,[8] based on resonant two-photon ionization in conjunction with time-of-flight mass spectrometric detection of the large VDW ions. The fluorescence studies (1)-(3) were conducted in free supersonic jets, while ion spectroscopy method (4) was carried out in skimmed jets.

RESULTS AND DISCUSSION

ELECTRONIC EXCITATIONS OF VAN DER WAALS COMPLEXES

Fig. 1 shows small portions of the fluorescence excitation spectra of several large molecules in supersonic expansions of Ar. On the basis of spectroscopic studies of these molecules,[6,7,15,17] we can assign the electronic origin of the lowest spin-allowed $S_0 \rightarrow S_1$ electronic transition of the bare ultracold molecule, which is marked 0–0 in fig. 1. The satellite bands, appearing in the low-energy side of the 0–0 transition of the bare molecule, are characterized by the following features: (1) Their energies depend on the identity of the diluent rare gas (fig. 2). (2) Their intensities exhibit a strong dependence on the stagnation pressure (fig. 3). (3) At higher pressures the spectral feature at lower energies become more prominent. All the spectral features appearing on the low-energy side of the electronic origin of the bare molecules (fig. 1 and 2) are assigned to $S_0 \rightarrow S_1$ electronic excitations of MR_n molecules. Such an inter-

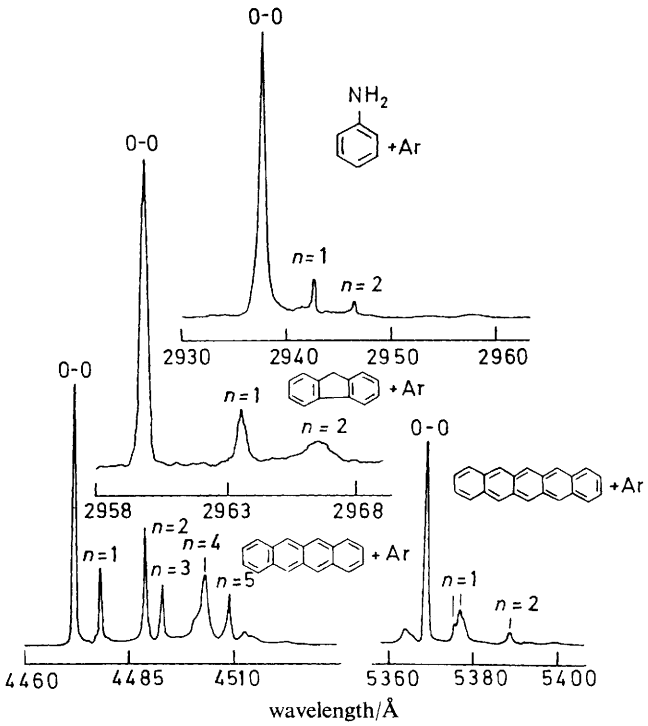

FIG. 1.—Fluorescence excitation spectra of the $S_0 \rightarrow S_1$ electronic origin of several bare molecules, M, and MAr_n complexes in supersonic expansions of Ar. The spectra were obtained under the following conditions: (1) aniline + Ar: continuous expansion from a 50 μm nozzle at pressure $p = 1060$ Torr and temperature $T = 70$ °C; (2) fluorene + Ar: pulsed expansion from a 35 mm × 0.2 mm nozzle slit at $p = 150$ Torr and $T = 105$ °C; (3) tetracene + Ar: continuous expansion from a 150 μm nozzle at $p = 609$ Torr and $T = 200$ °C; (4) pentacene + Ar: continuous expansion from a 200 μm nozzle at $p = 295$ Torr and $T = 280$ °C. The electronic origin of the bare molecule is marked as 0–0 and the coordination numbers of the MR_n complexes are marked.

pretation is borne out by the spectroscopic diagnostic methods, which will now be considered.

SPECTROSCOPIC DIAGNOSIS

The following spectroscopic diagnostic methods were utilized for the identification and characterization of the individual spectral features, which could unambiguously be assigned to distinct MR_n VDW molecules.

(A) COMPLEXATION OF BARE MOLECULES BY RARE GASES

We have followed the reduction of the intensity [M] of the 0–0 transition of a bare molecule by increasing the stagnation pressure. As is evident from fig. 4 and 5, [M] obeys the relationship

$$[M] = [M]_0 \exp(-K_1 p^2).$$

Thus, the attachment of the first R atom to a large aromatic molecule proceeds *via* a three-body collision

$$M + R + R \xrightarrow{K_1} MR_1 + R.$$

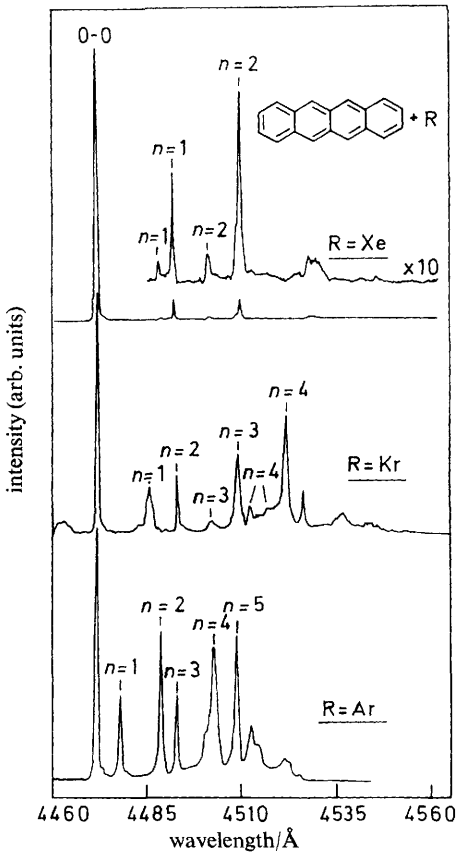

FIG. 2.—The fluorescence excitation spectra of tetracene–R_n (R = Ar, Kr and Xe) in continuous supersonic expansion of rare gases. Tetracene at 200 °C (vapour pressure 0.1 Torr) was mixed with Ar (p = 710 Torr), Kr (p = 465 Torr) or Xe (p = 181 Torr) and expanded through a 150 μm nozzle. The electronic origin of the bare molecule is marked as 0–0 and the coordination numbers of the tetracene–R_n complexes are marked.

It is interesting to note that even for the huge pentacene molecule, which is characterized by 102 vibrational degrees of freedom, " sticky " two-body collisions are ineffective in the stabilization of a longlived complex, and three-body collisions are necessary. The three-body mechanism is universal, applying to complexation of diatomics [18] and to huge molecules.

(B) PRESSURE DEPENDENCE OF THE INTENSITIES

The relative intensities of the spectral features attributed to individual MR_n VDW molecules were found to exhibit a pressure dependence of the form p^{2n} at low values of the stagnation pressure.[4,5] Such p^{2n} power law [18] reflects a three-body recombination mechanism for the formation of higher MR_n complexes

$$MR_{n-1} + R + R \xrightarrow{K_n} MR_n + R$$

where K_n is the three-body rate constant. Provided that these rates K_n are weakly dependent on n, we can invoke a " democratic assumption", setting $K_n = K$ for all n. The distribution of the MR_n complexes is then Poissonian, with the distribution para-

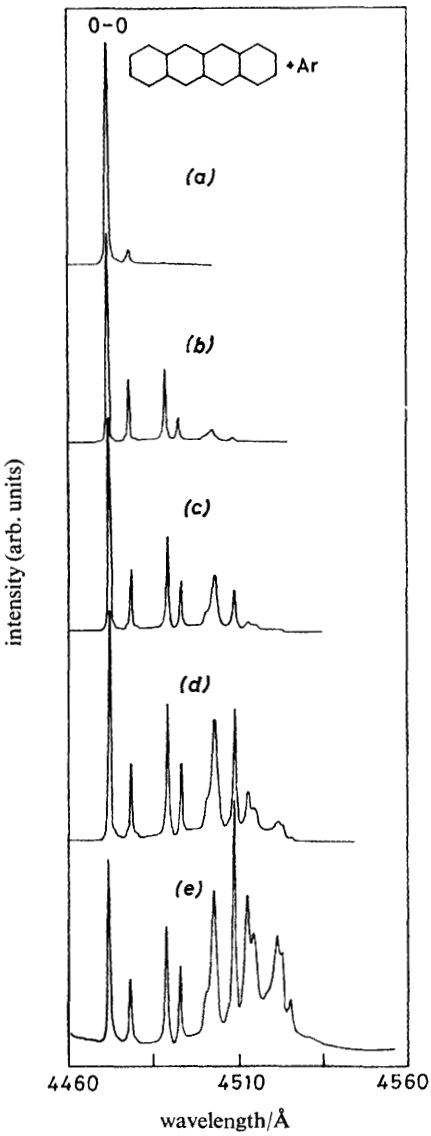

FIG. 3.—Fluorescence excitation spectra of the $S_0 \rightarrow S_1$ electronic origin of tetracene and of tetracene–Ar_n complexes in a continuous supersonic expansion through a 160 μm nozzle. The backing pressures of Ar are (*a*) 180, (*b*) 478, (*c*) 609, (*d*) 710 and (*e*) 853 Torr. The vibrationless 0–0 of the bare tetracene molecule is marked.

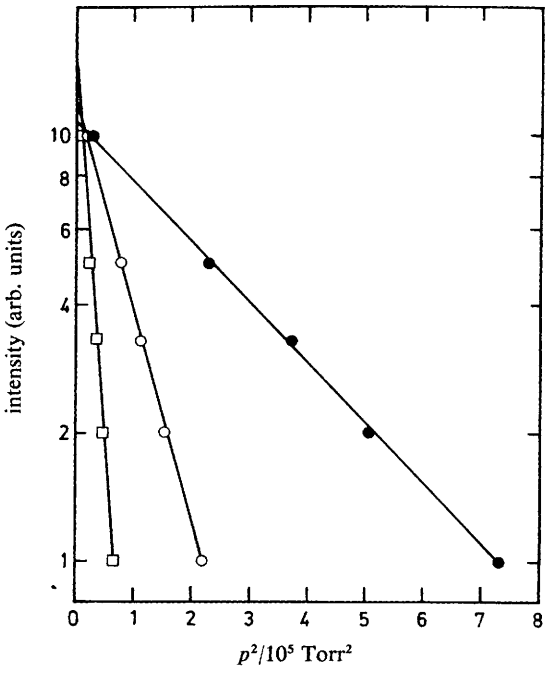

FIG. 4.—Dependence of the intensity [T] of the 0–0 transition of the bare tetracene molecule on the stagnation pressure, p, of the rare gas in a continuous expansion in Ar (●), Kr (○) and Xe (□) through a 150 μm nozzle. The nozzle temperature was 220 °C. The tetracene pressure was maintained constant in all experiments $[T] = [T_0] \exp(-kp_0^2)$.

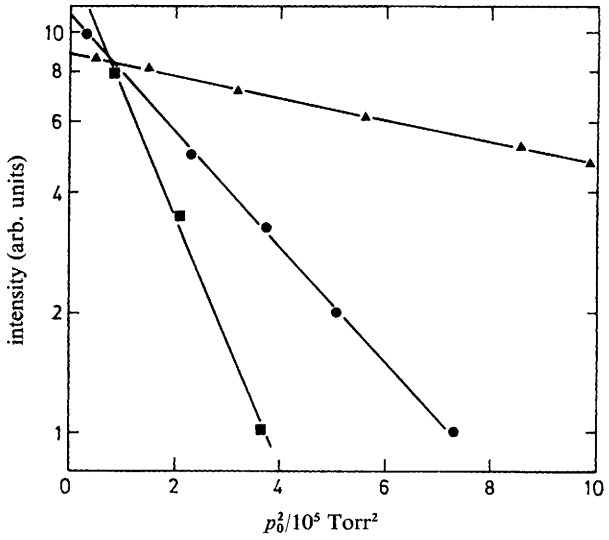

FIG. 5.—Dependence of the intensity of the 0–0 transition of the bare aniline, tetracene and pentacene molecules in continuous supersonic expansions of Ar on the stagnation pressure: ▲, aniline–Ar, $T = 70$ °C, $D = 50$ μm; ●, tetracene–Ar, $T = 220$ °C, $D = 150$ μm; ■, pentacene–Ar, $T = 280$ °C, $D = 200$ μm.

meter being Kp^2. The mean value of the complex size is $\langle n \rangle = Kp^2$, while the variance of the distribution is $\Delta n = K^{\frac{1}{2}}p$. The relative spectral intensity $[MR_n]$ of MR_n is given by

$$[MR_n]/[M] = (Kp^2)^n.$$

This relation was utilized for the analysis of the spectral features of tetracene–Ar_n and of tetracene–Kr_n complexes, which are portrayed in fig. 6 and 7. Seven distinct

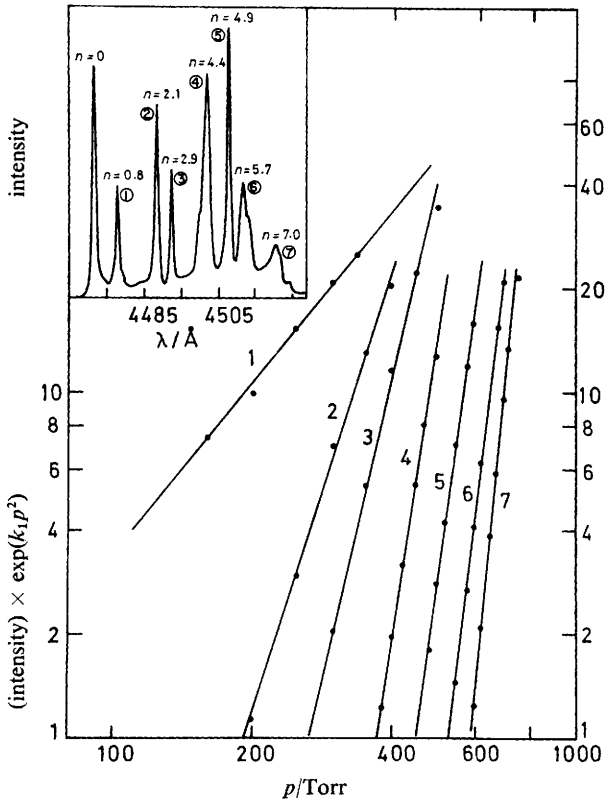

FIG. 6.—Dependence on the Ar pressure of the normalized intensities [tetracene–Ar_n]/[tetracene] = [tetracene–Ar_n] exp(K_1p^2) of the spectral features of the tetracene–Ar_n molecules, normalized by the intensity of the bare molecule, for supersonic expansions of tetracene in Ar. The upper insert shows the fluorescence excitation spectrum of tetracene seeded in Ar expanded at $p = 710$ Torr. The individual spectral features are labelled by the indices $j = 1, 2 \ldots 7$ in the order of increasing wavelength. The pressure dependence of the normalized intensities of these spectral features is of the form p^{2n}. The values of n obtained from this analysis are shown in the spectrum (upper insert).

spectral features in the tetracene–Ar system were assigned to excitations of tetracene–Ar_n complexes with coordination numbers $n = 1 \ldots 7$, while seven spectral features in the tetracene–Kr system could be attributed to excitations of tetracene–Kr_n complexes with $n = 1 \ldots 4$, with several distinct features corresponding to each of the chemical compositions, tetracene–Kr_3 and tetracene–Kr_4.

(C) ORDER OF APPEARANCE OF THE SPECTRAL FEATURES

The order of appearance of the excitations of the MR_n complexes with increasing p is expected to be sequential, starting with the spectral features due to excitations of

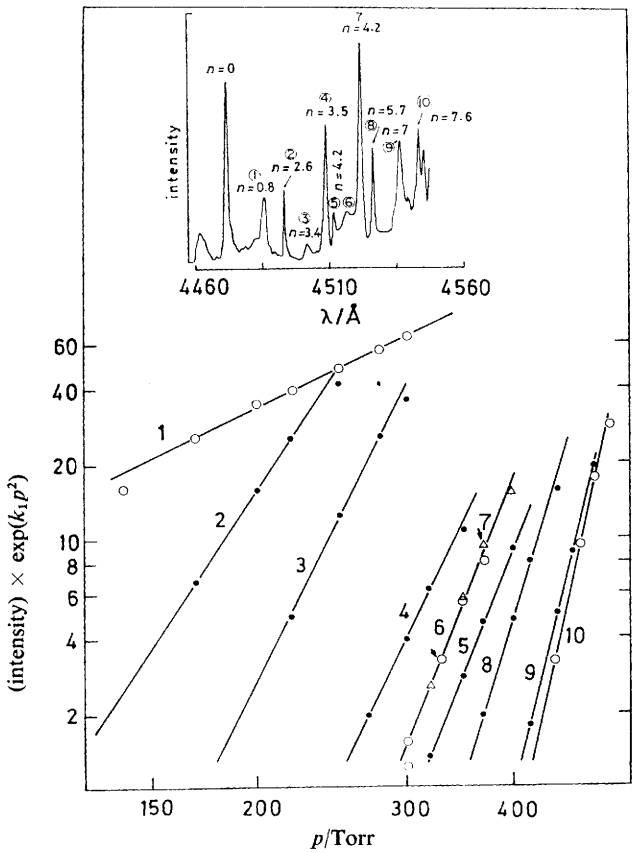

FIG. 7.—Dependence on the Kr pressure of the normalized intensities [tetracene–Kr_n]/[tetracene] = [tetracene–Kr_n] exp($-K_1p^2$) of the spectral features of tetracene–Kr_n molecules, normalized by the intensity of the bare molecule, for supersonic expansions of tetracene in Kr. The upper insert shows the fluorescence excitation spectrum of tetracene seeded in Kr expanded at $p = 465$ Torr. The individual spectral features are labelled by the indices $j = 1 \ldots 10$ in the order of increasing wavelength. The pressure dependence of the normalized intensities of these spectral features is of the form p^{2n}. The values of n obtained from this analysis are shown on the spectrum (upper insert).

the complexes with $n = 1$, while, at higher values of p, complexes characterized by higher coordination numbers will be exhibited. This qualitative criterion has been extremely useful in the identification of MR_n complexes with low n (=1-3) values.

(D) RESONANT TWO-PHOTON IONIZATION OF VDW MOLECULES

The laser-induced fluorescence techniques (A)-(C) are applicable only to prominent absorption bands of fluorescent complexes. The utilization of tuneable laser two-photon ionization (2PI) method [19-21] to VDW molecules, combined with time of flight mass spectroscopy of the resulting MR_n^+ ions,[8] provides an unambiguous identification of the detailed spectral features of MR_n complexes. We applied the resonant 2PI method for the spectroscopy of fluorene–Ar_n ($n = 1$-3) complexes. Fig. 8 shows the mass-resolved ion signal spectra of fluorene and of fluorene–Ar_n^+ ($n = 1$-3) ions. These energy-resolved and mass-resolved spectra monitor the spectral features of the

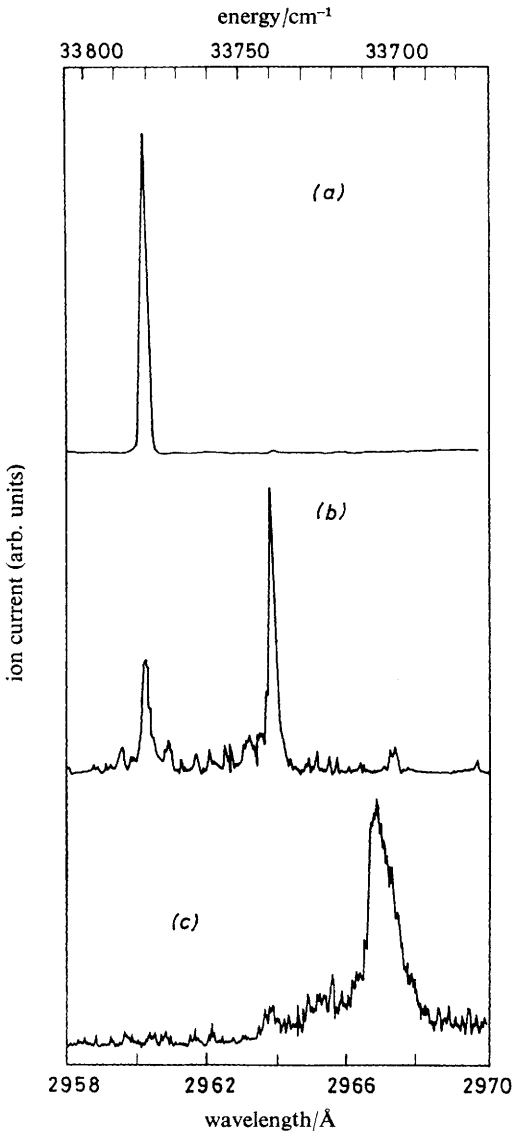

FIG. 8.—Ion current plotted against laser wavelength of fluorene$^+$ (*a*, $m/e = 166$), fluorene–Ar$^+$ (*b*, $m/e = 206$) and fluorene–Ar$_2^+$ (*c*, $m/e = 246$). Fluorene at 100 °C (vapour pressure 1.4 Torr) was seeded into Ar at $p = 1200$ Torr and expanded through a 300 μm pulsed nozzle. The jet was skimmed and photoionized by the laser in the ion source of a time-of-flight mass spectrometer.

intermediate resonant states, which involve the vibrationless $S_0 \rightarrow S_1$ excitations of individual fluorene–Ar$_n$ molecules. As is evident from table 1, there is an excellent agreement between the prominent features in the fluorescence excitation spectra and the ion current spectra of fluorene–Ar$_n$ complexes, providing conclusive evidence for the assignment of the spectral features of these large VDW molecules. In addition, the resonant 2PI method unveils some additional weak spectral features of the complexes which are obscured in the fluorescence spectra, providing information on the multiplet structure of these electronic excitations. Finally, it is worthwhile to note

TABLE 1.—EXCITATION ENERGIES OF FLUORENE–R_n COMPLEXES (IN cm^{-1}) [a-d]

molecule	mass-resolved resonant two-photon ionization	laser-induced fluorescence
fluorene	0	0
fluorene–Ar_1	−1(W) −41	−41
fluorene–Ar_2	−76	−75
fluorene–Ar_3	−118	−120
fluorene–Kr_1	−33(W) −63	−33(W) −63

[a] Energies (in cm^{-1}) represent spectral shifts from the electronic origin of the bare molecule. Negative signs correspond to red shifts. [b] The origin of the bare molecule determined by mass-resolved resonant 2PI is at 2960.2 ± 0.1 Å, which is in agreement with the laser-induced fluorescence method and which gives 2960.0 ± 0.1 Å. The absolute accuracy of wavelength scale is ±0.5 Å. [c] Accuracy of spectral shifts is ±1.5 cm^{-1}. [d] The weak satellite bands are denoted by (W).

TABLE 2.—EXCITATION ENERGIES $\delta\nu$ OF MR_n COMPLEXES RELATIVE TO THE 0–0 TRANSITION OF M (ENERGIES GIVEN IN cm^{-1}) [a-c]

Van der Waals complex	$n = 1$	$n = 2$	$n = 3$	$n = 4$	interrogation method
aniline–Ne_n	−4.8	−9.6			(B),(C)
aniline–Ar_n	−57	−102			(A), (B), (C)
fluorene–Ar_n	−41 −1(W)	−76	−118		(C), (D)
fluorene–Kr_n	−63 −33(W)				(C), (D)
fluorene–Xe_n	−113 −73(W) −63				(D)
tetracene–Ar_n	−35	−88	−109	−155	(A), (C)
tetracene–Kr_n	−70	−110	−186 −150(W)	−248 −223(W) −200(W)	(A), (C)
tetracene–Xe_n	−101 −83(W)	−189 −147(W)			(A), (C)
pentacene–Ar_n	−29 −25	−70			(A), (C)
pentacene–Kr_n	−62 −55	−86			(A), (C)

[a] Negative signs of $\delta\nu$ denote red spectral shifts. [b] The accuracy of the $\delta\nu$ values is ±2 cm^{-1} for aniline and fluorene complexes and ±4 cm^{-1} for tetracene and pentacene complexes. [c] When multiple spectra, corresponding to MR_n complexes with a fixed value of n, are exhibited, all the peak energies are listed. The weak satellite bands are labelled as (W).

that resonant 2PI *via* the electronic origin of these VDW molecules results in the photoselective production of large VDW ions, which are of considerable interest.

Table 2 summarizes the energies of the lowest excitation of MR_n molecules, each being given relative to the 0–0 transition of the corresponding bare M molecule. Only those features which were definitely identified using the spectroscopic diagnostic methods were included. These spectral features provide a rather comprehensive picture of the electronic excitations of MR_n, which do not change the internal vibrational state of M. These spectroscopic data provide a characterization of the composition of large VDW molecules. These " chemical type " data will now be supplemented with some crude information regarding potential surfaces to elucidate some features of the structure and intermolecular nuclear motion in these complexes.

MODEL POTENTIALS

One approach towards the elucidation of the structure and nuclear vibrational motion of large VDW molecules rests on model calculations of the intermolecular interactions. The potential surfaces of aromatic–rare-gas complexes were constructed [9] as a superposition of pairwise atom–atom potentials, the R–carbon atom pair potentials being taken from the heats of adsorption of rare-gas atoms on graphite,[22] the R–hydrogen atom pair potentials were estimated using empirical combination rules [23] and the R–R interaction pair potentials were represented in the conventional 6-12 form.[23] Fig. 9 and 10 provide a view of the potential surfaces of tetracene–Ar_1

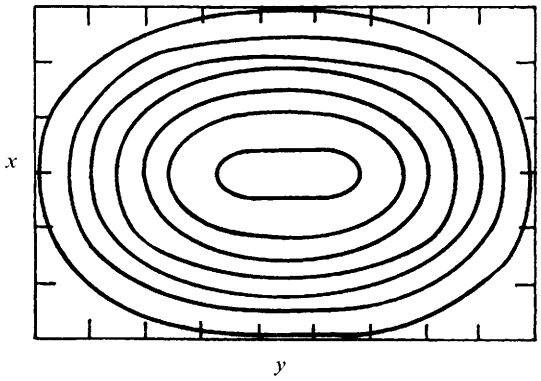

FIG. 9.—Contour map for the tetracene–Ar_1 potential in the plane parallel to the aromatic plane at the distance $z = 3.45$ Å from it. The innermost contour is at $E = -1.5$ kcal mol^{-1} and subsequent contour intervals are separated by 0.2 kcal mol^{-1}.

and of ovalene–Ar_1 parallel to the molecular xy plane at a distance of $z = 3.45$ Å away from it. Details of the potential surface of MR_1 complexes are portrayed in fig. 11 for tetracene–R_1 and in fig. 12 for pentacene–R_1 complexes. The following notable features of the potential surfaces of MR_1 complexes, consisting of a rare-gas atom bound to a linear polyacene, should be noted. First, the motion parallel to the short molecular axis x is characterized by a single potential minimum for all polyacenes. Secondly, the potential for motion parallel to the long molecular axis is characterized by several minima or inflection points, whose number is equal to the number of aromatic rings. Thirdly, for complexes containing an even number of aromatic rings, there are two equivalent points of minimum energy on each side of the molecule, which give rise to " tunnelling type " motion of the R atom. Fourthly, for complexes containing

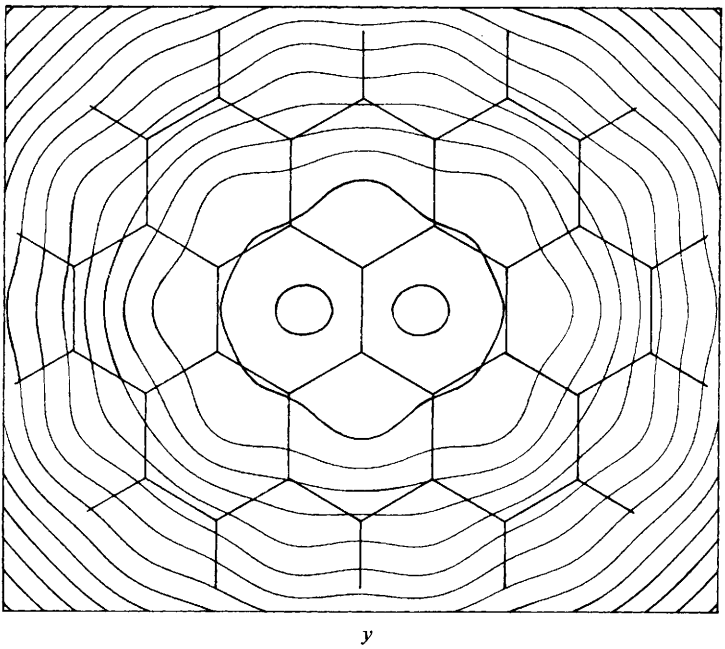

FIG. 10.—Contour map for the ovalene–Ar_1 potential in the plane parallel to the aromatic plane at the distance of $z = 3.45$ Å from it. The innermost contour is at $E = -1.80$ kcal mol^{-1} and subsequent contour intervals are separated by 0.10 kcal mol^{-1}.

an odd number of rings, *i.e.* benzene, anthracene and pentacene, there is a single absolute minimum energy on each side. Fifthly, for the large odd-ringed pentacene, there are two energetically close but distinct potential minima on each side, differing by *ca.* 10 cm^{-1}. Sixthly, the R atom parallel to the molecular plane exhibits large amplitude non-harmonic motion. Seventh, the potential energy for the motion of the R atom away from the molecular plane for all these polyacene complexes exhibits a universal form, which is close to the familiar 6-12 potential. Most of these gross features of the potential surfaces are determined essentially by the topology of the interaction.

We now turn to somewhat less reliable numerical results pertaining to the ground-state energetics and structure. Table 3 summarizes the energies of the potential minima, which provide an estimate of the ground-state binding energies for a variety of complexes. The intermolecular equilibrium separation r_0 and the frequency ν for the motion of R with respect to the molecular plane are summarized in table 4 for tetracene–R_1 molecules, being characteristic for all of these large complexes.

Similar model calculations provided information [9] on the equilibrium structure of MR_n complexes containing several rare-gas atoms, which will briefly be considered in relation to the cardinal question concerning the existence of isomers. Regarding MR_2 complexes of large polyacenes, one can argue, without alluding to any numerical calculations, that the binding of two R atoms to a large aromatic molecule will result in an energetically favoured configuration, with the two R atoms being located on the same side of the aromatic ring. This single-sided structure is stabilized by the attractive interaction between the pair of the R atoms. This expectation is borne out by numerical calculations for tetracene–R_2 molecules (R = Ar, Kr and Xe), where the stabilization energy of the one-sided structure relative to the two-sided configuration

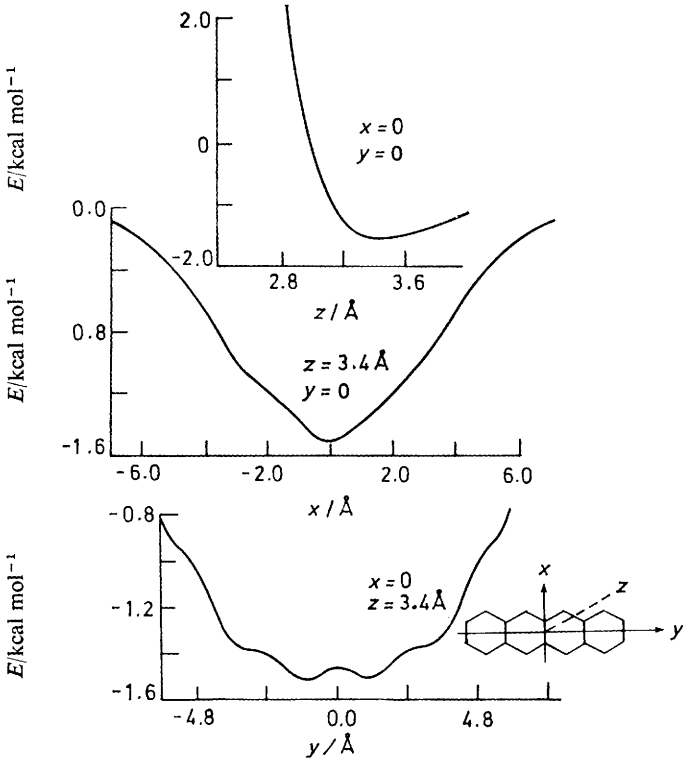

FIG. 11.—Tetracene–Ar_1 potential along the x, y and z axes.

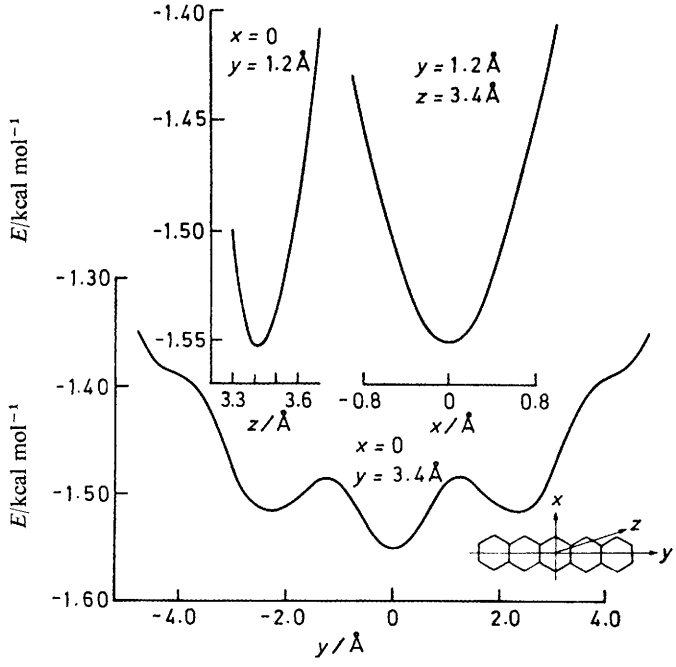

FIG. 12.—Pentacene–Ar_1 potential along the x, y and z axes.

TABLE 3.—DISSOCIATION ENERGIES FROM THE MINIMA OF MODEL POTENTIALS FOR MR_1 COMPLEXES (ENERGIES GIVEN IN cm^{-1}) [a-c]

M \ R	Ar	Kr	Xe
benzene	393 [2]	458 [2]	545 [2]
anthracene	519 [2]	612 [2]	753 [2]
tetracene	531 [4]	630 [4]	777 [4]
pentacene	542 [2]	644 [2]	798 [2]
	(533) [4]	(633) [4]	(783) [4]
ovalene	638 [4]	762 [4]	962 [4]

[a] The contribution of the zero-point energy of M–R motion to the dissociation energy is neglected. [b] For benzene, anthracene, tetracene and ovalene, a single value of the minimum energy is exhibited. In the case of pentacene, two minima appear in the potential surfaces, the energy of the second minimum being given in round brackets. [c] Number of points of minimum energy are given in square brackets.

is *ca.* 40-60 cm^{-1}. Accordingly, at low temperatures a single equilibrium configuration is expected to be energetically favoured, and no isomers are expected for tetracene–R_2 complexes. The situation is more complicated and interesting for MR_3 complexes. Model calculations for tetracene–R_3 complexes raise the distinct possibility of the

TABLE 4.—ESTIMATES OF FREQUENCY (ν), DISSOCIATION ENERGY (D), NUMBER OF BOUND VIBRATIONAL LEVELS ($\mathscr{H}$) AND EQUILIBRIUM DISTANCES (r_0) FOR THE PERPENDICULAR VIBRATIONAL MOTION OF A RARE-GAS ATOM IN TETRACENE–R_1 COMPLEXES

rare gas	ν/cm^{-1}	D/cm^{-1}	$\mathscr{H}$	r_0/Å
Ar	57	531	18	3.45
Kr	45	630	28	3.45
Xe	41	777	38	3.70

peaceful coexistence of two isomers, a two-sided structure and a triangular same-sided configuration, whose energies are very close.[9] Such a pattern of nearly isoenergetic isomers is expected to be exhibited for large MR_n complexes, which are characterized by a high coordination number $n > 3$.

DISSOCIATION ENERGIES

The model calculations of the preceding section indicate that the binding energies, D, of R atoms to aromatic molecules are relatively large. Pertinent experimental information regarding these binding energies was obtained from three sources:

(1) Resonant 2PI of a MR_1 complex, proceeding *via* an intermediate excitation of an intramolecular vibration in S_1, will result in the M^+ ion when the vibrational predissociation (VP) channel is open in the intermediate state while, when the VP channel is closed, extensive production of the MR_1^+ ion is expected. This approach was utilized [8] to set upper and lower bounds on D for fluorene–R_1 complexes.

(2) The lack of VP from an electronic–vibrational excitation of a MR_1 VDW complex, as interrogated by energy-resolved emission, indicates that the reactive channel

is presumably closed. This approach was used [4] to set a lower limit for D of tetracene–Ar_1.

(3) The heavy-atom effect on the decay lifetime of the S_1 state of VDW complexes was adopted [4] to search for the onset of VP in tetracene–Kr_n complexes, establishing both a lower and an upper limit for D.

Table 5 summarizes the experimental findings for the binding energies of R atoms to

TABLE 5.—EXPERIMENTAL ESTIMATES OF BINDING ENERGIES OF LARGE VAN DER WAALS COMPLEXES

complex	dissociation energy/cm^{-1}	method [a]
fluorene–Ar_1	$408 \leqslant D \leqslant 728$	(1)
tetracene–Ar_1	$D \geqslant 314$	(2)
tetracene–Kr_1	$314 \leqslant D \leqslant 1200$	(3)

[a] (1) Resonant 2PI, (2) energy-resolved emission, (3) vibrational predissociation interrogated by the external heavy-atom effect.

large aromatics in the S_1 state. To obtain estimates of the ground-state D values, these values should be corrected by the (small) difference in the binding energy between S_1 and S_0. These experimental estimates of D concur with the results of our model calculations.

MULTIPLE SPECTRA

The spectral features of an intramolecular vibrationless excitation of a MR_n complex, which corresponds to a single chemical composition (table 2), fall into two categories:

(1) A single broadened spectral feature is exhibited for the MR_n complex. This is the case for some large complexes, *i.e.* tetracene–Ar_n ($n = 1$ and 2) and tetracene–Kr_n ($n = 1$ and 2). Our model calculations predict that for tetracene–R_1 and tetracene–R_2 complexes only a single chemical isomer is energetically stable, which is in accord with the experimental data.

(2) A multiple spectrum is exhibited with several distinct spectral features for a MR_n complex(es) with a fixed n. This state of affairs prevails for tetracene–Xe_n ($n = 1$ and 2), tetracene–Kr_3 and tetracene–Kr_4, fluorene–R_1 (R = Ar, Ke and Xe) and pentacene–R_n (R = Ar, Kr and $n = 1,2$).

The broadening of the spectral features and the appearance of multiple spectra can originate from the following causes:

(A) The existence of nearly isoenergetic chemical isomers. The two separate spectral features in the spectrum of tetracene–Kr_3 are assigned to the existence of two isomers. These are characterized by a two-sided configuration and by a one-sided triangular configuration. The three distinct spectral features of tetracene–Kr_4 are also tentatively assigned to distinct chemical isomers, as implied by the model calculations presented earlier in this paper.

(B) Thermal population of intermolecular M–R vibrational states in S_0, resulting in hot bands and in sequence bands involving low-frequency modes. The broadening of the spectral features of tetracene–R_1 and tetracene–R_2 (R = Ar and Kr) may be due to this effect.

(C) The existence of several conformers. When the potential surface of the complex is characterized by two or more close lying but non-degenerate minima, the

vibrational structure will consist of several close lying levels. Thermal populations of such vibrational states, which prevail even at the low temperatures attained in supersonic expansions, are expected to result in several distinct vibrational excitations. Vibrational conformers differ from isomers [case (A)], as in the latter case the potential barrier separating the different structures is very large. Conformer splitting is expected to be exhibited by the odd-ringed pentacene–R_1 complex (fig. 12). The multiple doublet spectra of pentacene–Ar_1 and of pentacene–Kr_1 [5] (table 2) are tentatively attributed to conformers, whose minimum energies are separated by *ca.* 10 cm^{-1}.

(D) Vibrational structure due to M–R intermolecular motion in the S_1 state. This will be amenable to observation, provided that the relevant intermolecular vibrational frequency is sufficiently high and that the Franck–Condon vibrational overlap is favourable. Such vibrational structure is expected to be exhibited towards higher energies from the main vibrationless peak. The vibrational frequency for out-of-plane motion of R in MR_n is 40-50 cm^{-1} (table 4), being amenable to observation. The weak secondary features in tetracene–Xe_n (n = 1 and 2) and in fluorene–R_1 (R = Ar, Kr and Xe) correspond to excitations of 30-50 cm^{-1} and are tentatively attributed to intermolecular vibrational excitations in S_1, which are in accord with the model calculations.

MICROSCOPIC SPECTRAL SHIFTS

The energetic shift, $\delta\nu$, of the electronic origin of the $S_0 \rightarrow S_1$ excitation of a well-characterized MR_n VDW complex relative to the 0–0 transition of the bare M molecule corresponds to the spectral shift induced by a well-defined microscopic solvent structure. The quantitative data for these spectral shifts (table 1) of aromatic hydrocarbons exhibit the following features:

(1) The spectral shifts induced by Ne, Ar, Kr and Xe atoms are all towards lower energies. Such red spectral shifts are assigned conventionally to the change in dispersive interactions.[24] It is a quite simple matter to extend the Longuet-Higgins–Pople formalism [24] to large MR_n complexes bypassing the dipole–dipole expansion by the use of a multicentre monopole expansion.[25] The red dispersive spectral shift for MR_1 can be expressed in the form $\delta\nu_{dis} = \alpha F(\{R_{\alpha\beta}\}\{x_\alpha\},\{y_\alpha\},\{C_{j\alpha}\},\{E_{jk}\},\bar{E})$, where α is the polarizability of the R atom, $R_{\alpha\beta}$ is the distance between the αth C atom located at $(x_\alpha,y_\alpha,z_\alpha = 0)$ and the R atom, $\{C_{j\alpha}\}$ are the molecular-orbital coefficients, $\{E_{jk}\}$ are $\pi \rightarrow \pi^*$ excitation energies, $\bar{E}$ stands for an average excitation energy of R, while the explicit form of the function $F(\ )$ is derived by second-order perturbation theory.

(2) The microscopic spectral shifts exerted by a single R atom reveal a linear dependence on the polarizability of the perturbing atom $\delta\nu_{dis} \propto \alpha$ (fig. 13) as is expected for dispersive interactions.

(3) The spectral shifts of MR_n complexes are only approximately additive per added R atom (fig. 14). Deviations of the order of 10-20% from additivity of $\delta\nu_{dis}$ do not seem to originate from three-body dispersive interactions, but rather from the occupation of geometrically inequivalent sites by the successive R atoms, which complex with M.

The dependence of $\delta\nu$ on the nature of the electronic excitation of the aromatic hydrocarbon has not yet been elucidated. In general, one expects that the dispersive contribution to $\delta\nu$ will increase with increasing oscillator strength, f, of the electronic transition.[24,25] This expectation is borne out by the observation of small spectral shifts for the $S_0 \rightarrow S_1$ transition of ovalene–R_n (R = Ar and Kr) complexes [6]

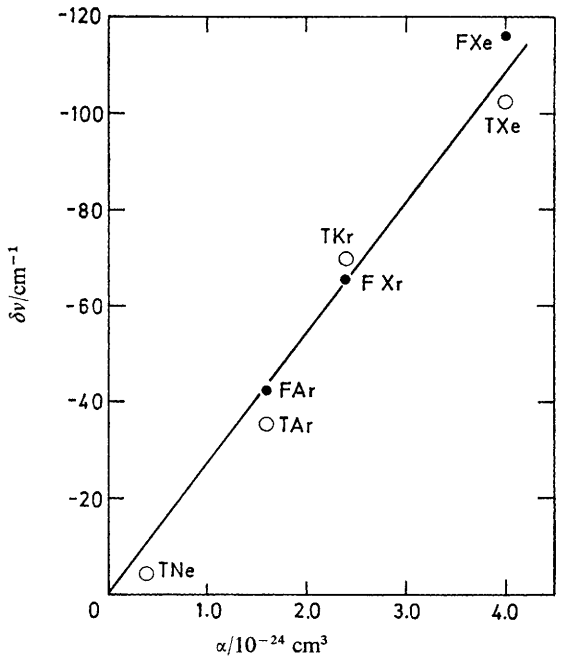

FIG. 13.—Dependence of the red spectral shifts $\delta\nu$ of the vibrationless $S_0 \rightarrow S_1$ excitations of tetracene–R_1 and fluorene–R_1 (R = Ne, Ar, Kr and Xe) molecules on the polarizability α of the rare-gas atom. The solid straight line, which passes through the origin, corresponds to the relation $\delta\nu = A\alpha$. The proportionality constants A are very close for the two families of complexes; however, other MR_1 families are expected to be characterized by different A values.

(with $f \approx 10^{-3}$), which are considerably lower than the $\delta\nu$ values for tetracene–R_n complexes (where $f \approx 10^{-1}$).

In complexes consisting of alternating non-substituted hydrocarbons bound to heavy rare-gas atoms, the dispersive contribution to $\delta\nu$ is expected to dominate. An additional electrostatic contribution to $\delta\nu$, originating from dipole–induced-dipole interactions (DIDI) is expected to be exhibited for complexes containing polar molecules, which undergo an appreciable change in their dipole moment upon electronic excitation. This is the case for aniline–Ar_n (n = 1 and 2) complexes, where the dipole moment of the aniline molecule is 1.5 D * in S_0 and 2.4 D in S_1.[26] The aniline–Ar_n complexes exhibit a large red spectral shift (table 1). We have adopted a simple electrostatic model for the evaluation of the contribution $\delta\nu_{DIDI}$ from DIDI to $\delta\nu$ using the π electron density in the S_0 and S_1 states [26] and locating the Ar atom at 3.45 Å above the centre of the ring, resulting in $\delta\nu_{DIDI} \approx -4$ cm^{-1}. This contribution from DIDI is in the right direction; however, the major contribution to $\delta\nu$ originates from dispersive terms.

An additional contribution to $\delta\nu$ for $S_0 \rightarrow S_1$ transitions is expected to originate from short-range repulsive interactions in S_1, which result in spectral shifts to higher energies. For He and Ne complexes dispersive interactions are weak and these repulsive interactions are important. Blue spectral shifts exhibited for He complexes essentially originate from this effect.

Up to this point spectral shifts were considered within the framework of a frozen nuclear picture. The possible effects of nuclear motion on $\delta\nu$ are intriguing in this

* 1 D $\approx 3.33356 \times 10^{-30}$ C m.

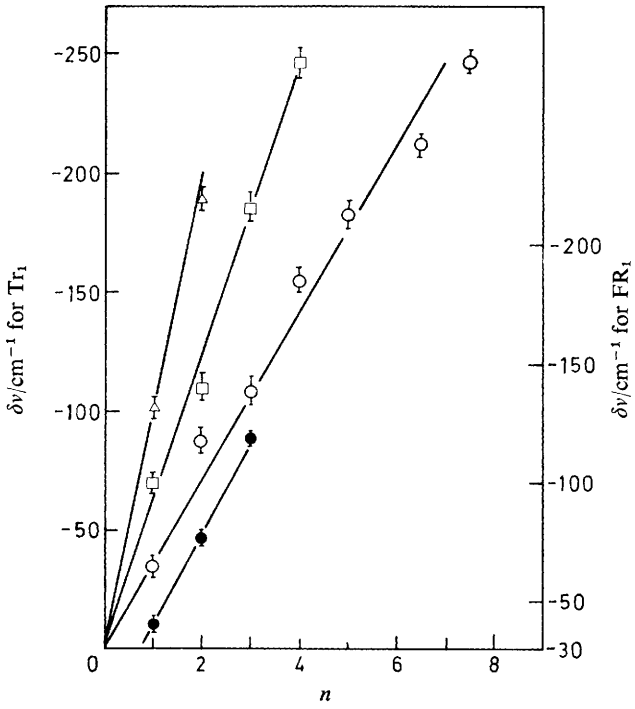

FIG. 14.—Dependence of the red spectral shifts $\delta\nu$ of the vibrationless $S_0 \rightarrow S_1$ excitations of the tetracene–R_n [R = Ar (○), Kr (□) and Xe (△)] and of the fluorene–Ar_n (●) molecules on the coordination number n. The straight lines are provided for the sake of a visual demonstration of the additivity of the spectral shifts per added R atom.

context. The simplest effect in this category involves the modification of the vibrational frequencies in MR_n, relative to those of the bare molecule. We are not aware of any information concerning this effect.

INTRAMOLECULAR DYNAMICS

Interstate and intrastate intramolecular dynamics of MR_n complexes are of intrinsic interest for the understanding of the effects of external perturbations on electronic relaxation phenomena and for the elucidation of the nature of internal energy flow in weakly bound systems.

The exploration of interstate dynamics of VDW molecules provides information on microscopic solvent perturbations on electronic relaxation (ER) from photoselected states of well-characterized MR_n complexes. A prediction [28] of the theory of intramolecular ER in large molecules, corresponding to the statistical limit, is that the ER rate of the electronic origin is practically unaffected by an " inert " solvent, which does not modify the energy levels and the intramolecular coupling. As is apparent from the lifetime data assembled in table 6, the lifetimes τ of the vibrationless S_1 excitations of tetracene–Ne_1, tetracene–Ar_n (n = 1-4) and pentacene–Ar_n (n = 1 and 2) complexes are close to and somewhat longer than the lifetime τ_0 of the S_1 origin of the corresponding bare molecules, which is in accord with theory.[28] On the other hand, the lifetimes of tetracene–Kr_n, pentacene–Kr_n and tetracene–Xe_n reveal a dramatic shortening of τ relative to τ_0 (table 6). This is attributed to the external heavy-atom effect (EHAE) on

TABLE 6.—DECAY LIFETIMES FROM THE VIBRATIONLESS S_1 STATE OF MR_n MOLECULES

molecule [a]	τ/ns [b]
T	19
TNe_1	33
TAr_1	29
TAr_2	35
TAr_3	17
TAr_4	21
TAr_5	27
TAr_6	21
TAr_7	26
TKr_1	7
TKr_2	8
TKr_3	9
TKr_4	9
TXe_1	<3
TXe_2	<3
P	19
PAr_1	22
PAr_2	19
PKr_1	6

[a] T = tetracene, P = pentacene; [b] accuracy of lifetimes $\pm 10\%$.

the $S_1 \rightarrow T_1$ intersystem crossing [3,4] manifesting the modification of the non-adiabatic coupling in M. Two scrambling mechanisms inducing the EHAE can be operative,[29] *i.e.* (I) mixing with neutral excitations of the heavy R atom, and (II) mixing with charge transfer states. Mechanism (I) is cumulative with respect to n, while mechanism (II) is determined by M–R pair interactions. The observation (table 6) that the lifetimes of tetracene–Kr_n (n = 1-4) molecules are very close, showing only a slight variation with increasing n, implies that for these complexes mechanism (II) is dominating.

The understanding of intrastate reactive vibrational predissociation (VP) [28] and non-reactive vibrational energy flow [28] in large MR_n complexes is still in the embryonic stage. In a vibrationally excited MR_n VDW complex, characterized by a small value of n, the following mechanisms may be operative: (i) Non-reactive processes: when the intramolecular vibrational energy of M is lower than the binding energy of R, vibrational energy flow from M to the VDW bonds can occur. The low-frequency M–R modes may accept energy in small portions, as the vibrationally excited M molecule may cascade down *via* the intramolecular vibrational ladder. In view of the relatively high D values for $M–R_1$ complexes (table 2), this non-dissociative mechanism is operative for the 314 cm^{-1} vibrational excitation of tetracene–R_1 [4] (R = Ar and Kr). (ii) Reactive processes: when the intramolecular vibrational excitation of M exceeds D, reactive VP can occur, as demonstrated for tetracene–Kr complexes excited above 1200 cm^{-1}.[4]

For MR_n complexes with a large number of R atoms clustering around M, the mechanism of vibrational energy relaxation may undergo a qualitative change. Even when the intramolecular vibrational energy of M exceeds the M–R binding energy, non-dissociative vibrational relaxation can occur *via* energy transfer to the intermolecular " phonon modes " of the large cluster. This problem bears a close analogy to vibrational relaxation of a guest molecule in a host matrix, except that the matrix is of a finite size. It will be interesting to monitor the " transition " from a

reactive molecular-type VP process to a solid-state-type relaxation process with increasing coordination number of the complex. The notion of low-frequency "phonon modes" of large VDW complexes brings up some intriguing questions regarding the establishment of relations and correlations between the energetic and dynamic features of "free" large molecules and of these molecules in condensed phases. Studies of the energetics and dynamics of VDW complexes and of large molecules embedded in large clusters [30] will bridge the gap between these two cultures.

This research was supported in part by the United States Army through its European Research Office, and by the United States–Israel Binational Science Foundation (grant no. 2641), Jerusalem, Israel.

[1] D. H. Levy, *Annu. Rev. Phys. Chem.*, 1980, **31**, 197.
[2] D. H. Levy, in *Advances in Chemical Physics*, ed. J. Jortner, R. A. Levine and S. A. Rice (Wiley Interscience, New York, 1981), vol. 47, part I, p. 323.
[3] A. Amirav, U. Even and J. Jortner, *Chem. Phys. Lett.*, 1979, **67**, 9.
[4] A. Amirav, U. Even and J. Jortner, *J. Chem. Phys.*, 1981, **75**, 2489.
[5] A. Amirav, U. Even and J. Jortner, *J. Phys. Chem.*, 1981, **85**, 309.
[6] A. Amirav, U. Even and J. Jortner, *J. Chem. Phys.*, 1981, **74**, 3745.
[7] A. Amirav, U. Even and J. Jortner, *Chem. Phys.*, in press.
[8] S. Leutwyler, U. Even and J. Jortner, *Chem. Phys. Lett.*, in press.
[9] M. J. Ondrechen, Z. Berkovitch-Yellin and J. Jortner, *J. Am. Chem. Soc.*, 1981, **103**, 6586.
[10] T. R. Heyes, W. Henke, H. L. Selzle and E. W. Schlag, *Chem. Phys. Lett.*, 1980, **77**, 19.
[11] W. Klemperer, *Ber. Bunsenges. Phys. Chem.*, 1974, **78**, 128.
[12] K. V. Chance, K. H. Bowen, J. S. Winn and W. Klemperer, *J. Chem. Phys.*, 1979, **70**, 5157.
[13] K. C. Jackson, P. R. R. Langridge-Smith and B. J. Howard, *Mol. Phys.*, 1980, **39**, 717.
[14] A. Amirav, U. Even and J. Jortner, *Chem. Phys.*, 1980, **51**, 31.
[15] A. Amirav, U. Even and J. Jortner, *J. Chem. Phys.*, 1981, **75**, 3370.
[16] A. Amirav, U. Even and J. Jortner, *Chem. Phys. Lett.*, 1981, **83**, 1.
[17] A. Amirav, U. Even and J. Jortner, *Chem. Phys. Lett.*, 1980, **71**, 21.
[18] R.E. Smalley, L. Wharton and D. H. Levy, *J. Chem. Phys.*, 1977, **66**, 2750.
[19] A. Herman, S. Leutwyler, E. Schumacher and L. Wosto, *Helv. Chim. Acta*, 1978, **61**, 453.
[20] U. Boessel, H. J. Neusser and E. W. Schlag, *Z. Naturforsch., Teil A*, 1978, **33**, 1546.
[21] M. A. Duncan, T. G. Dietz and R. E. Smalley, *J. Chem. Phys.*, 1981, **75**, 2118.
[22] A. D. Crowell and R. B. Steele, *J. Chem. Phys.*, 1961, **34**, 1347.
[23] J. O. Hirschfelder, C. F. Curtiss and R. B. Bird, in *Molecular Theory of Gases and Liquids* (Wiley, New York, 1954), p. 168.
[24] H. C. Longuet-Higgins and J. A. Pople, *J. Chem. Phys.*, 1957, **27**, 192.
[25] C. A. Coulson and P. L. Davis, *Trans. Faraday Soc.*, 1952, **48**, 777.
[26] J. R. Lombardi, *J. Chem. Phys.*, 1969, **50**, 3780.
[27] R. E. Smalley and J. B. Hopkins, personal communication.
[28] J. Jortner and R. D. Levine, in *Advances in Chemical Physics*, ed. J. Jortner, R. D. Levine and S. A. Rice (Wiley Interscience, New York, 1981), vol. 47, p. 1.
[29] S. P. McGlynn, T. Azumi and M. Kimoshita, in *Molecular Spectroscopy of the Triplet State* (Prentice Hall, Engelwood Cliffs, N.J., 1969).
[30] A. Amirav, U. Even and J. Jortner, *Chem. Phys. Lett.*, 1980, **72**, 17.